

Evaluation of the Inhibition Effects of Natural Terpenoids on *Toxoplasma gondii* Tachyzoites

Zi-Yang Jiang

Department of Parasitology, West China School of Basic Medical Sciences and Forensic Medicine
Sichuan University,

Kai Dong

Department of Parasitology, West China School of Basic Medical Sciences and Forensic Medicine
Sichuan University,

Zheng-Song Huang

College of Chemistry, Sichuan University

Chang-Chun Yuan

College of Chemistry, Sichuan University

Bo Liu

College of Chemistry, Sichuan University

Qi-Wei Chen

Department of Parasitology, West China School of Basic Medical Sciences and Forensic Medicine
Sichuan University,

Jian-Ping Chen (✉ jpchen007@163.com)

Department of Parasitology, West China School of Basic Medical Sciences and Forensic Medicine
Sichuan University,

Research Article

Keywords: *Toxoplasma gondii*, apicomplexan parasites, apoptosis, host immune system, terpenoids, chlorajaponilide C

Posted Date: June 22nd, 2022

DOI: <https://doi.org/10.21203/rs.3.rs-1760835/v1>

License:  This work is licensed under a Creative Commons Attribution 4.0 International License.

[Read Full License](#)

Abstract

Background

At present, the preferred method for the clinical treatment of toxoplasmosis is still drug therapy such as pyrimethamine and sulfadiazine, but there are problems such as large side effects and drug resistance. Terpenoids are distributed in nature and a large number of studies have shown that they have effective inhibitory effects on various parasites.

Methods

In this study, we used small-molecule intermediate products of natural terpenoid *chlorajaponilide C* to evaluate their cytotoxicity and their intracellular and extracellular inhibitory effects on *Toxoplasma gondii* tachyzoites.

Results

We demonstrated that two of these target compounds could induce tachyzoite apoptosis probably by altering tachyzoite mitochondrial membrane potential, calcium homeostasis, and lipid metabolism, effectively reducing the number of extracellular tachyzoites. In addition, the two target compounds were also able to effectively clear intracellular tachyzoites, possibly enhancing this effect by interacting with the host cell's immune system.

Conclusions

Two terpenoid natural products with low cytotoxicity had direct and indirect anti-toxoplasma effects and were expected to further evaluate their potential for the treatment of toxoplasmosis.

Introduction

Toxoplasma gondii is a globally ubiquitous zoonotic apicomplexan parasite that can infect almost all kinds of warm-blood animal including human beings. Data showed that about 30% of the world's population suffered from toxoplasmosis, which was considered to be one of the most prevalent parasitic infections[1]. Felines are the definitive hosts of *T. gondii* and the only ones that shed oocysts. The main route of transmission of *Toxoplasma gondii* is foodborne way[2], that is, ingestion of tissue cysts in raw or undercooked meat of infected animals or ingestion of raw vegetables or water contaminated with oocysts. Toxoplasma infection in healthy adults is usually asymptomatic. However, neonatal or immunocompromised individuals with HIV infection, long-term treatment by corticosteroids, hematological malignancies, and transplant recipients can experience severe disease and even death after infection[3, 4, 5].

At present, the routine clinical treatment of toxoplasmosis includes pyrimethamine(pyrimethamine) combined with sulfadiazine and trimethoprim combined with sulfamethoxazole as well as spiramycin[6]. However, these regimens have the disadvantages of high toxicity or occurrence of relapse if long-term treatment is not adhered to[7]. Moreover, these regimens act only on acute infections, and have little effect on latent infections or central nervous system diseases caused by *T. gondii*[8, 9]. The emergence of drug resistance also increases the difficulty of treatment[10]. Therefore, the development of new drugs with high efficiency and low toxicity is one of the primary tasks for this pathogen.

Natural products have become an important source of drugs for clinical use. Herbal plants or plant extracts are usually safer than synthetic drugs for the treatment of parasitic diseases[11, 12]. Terpenoids, as the main structural components of many natural products with medicinal properties, can be extracted in large quantities from nature. In recent years, terpenoids and their derivatives had already been reported to achieve certain effects in the treatment of parasitic diseases. Zhang L H et al. synthesized various derivatives of Ursolic acid, a pentacyclic triterpenoid found in most plant species[13]. They demonstrated that Ursolic acid and its derivatives have good *in vitro* anti-*T. gondii* activity, and could effectively restore normal body weight in *T. gondii*-infected mice and reduce *in vivo* hepatotoxicity. The therapeutic effect of the derivatives was better than that of Ursolic acid, and the anti-Toxoplasma effect was achieved by inhibiting calcium-dependent protein kinase 1 (TgCDPK1). Darne P et al. studied the antiparasitic effect of lupane-type pentacyclic triterpenes isolated from black alder (*Alnus glutinosa*), found that Betulinone was highly active against *Toxoplasma gondii*, and identified its most likely target as TgCDPK3 [14]. The above studies have shown that terpenoids could achieve anti-parasitic effects through different ways, especially protozoa such as *T. gondii* and *Leishmania*.

In this article, we used the small-molecule intermediate products of natural terpenoid *chlorajaponilide C* to explore the effects of these compounds against *T. gondii* intracellularly and extracellularly, and the possible mechanism of action, providing possible options for the development of new anti-*T. gondii* drugs.

Materials And Methods

Drugs and chemicals

The 36 compounds to be screened were small-molecule intermediate products of natural terpenoid *chlorajaponilide C*, the synthesis of which had been reported previously[15]. 100 nM stock solutions of each compound were prepared in dimethyl sulfoxide (DMSO, MP biomedical, USA) and stored at -20°C. Pyrimethamine, azithromycin and staurosporine were purchased from MCE, USA.

Parasites strain

The type I virulent RH strain of *T. gondii* (generously donated by Guizhou Medical University, China) was used in this study. The RH strain was removed from liquid nitrogen and recovered in a water bath of 37°C for 30 min and then maintained *in vitro* by serial passage in human foreskin fibroblasts (HFF). When over

90% of the infected cells were lysed, the parasites were obtained together with the attached cells with a gentle scrape by a cell scraper, followed by centrifugation at 100×g for 10 min at 4°C before the supernatants were collected. Next, the mixture was passed through a 25-gauge syringe needle several times, centrifuged at 2,000×g for 10 min to remove the supernatants, and resuspended in either PBS (for infection) or RPMI 1640 medium (Gibco, USA) supplemented with 5% fetal bovine serum (Endo buffer) at 37°C in 5% CO₂ (for treatment).

Cells

A murine macrophage-stable cell line (RAW 264.7) was cultured at 37°C in a 5% CO₂/95% air mixture in RPMI 1640 medium containing 2.05 mM L-glutamine, Dulbecco's modified Eagle's medium (DMEM; Gibco, USA), respectively, supplemented with 10% fetal bovine serum (PAN, Germany) and 100 g/ml of antibiotics (penicillin and streptomycin; Ameresco, USA), with passage taking place every 3 to 4 days. When cells were over 80% confluent, 5 ml of trypsin with 0.25% EDTA and phenol red (Solarbio, China) was employed to digest the cells before they were washed off with fresh medium by pipetting for further seeding procedures.

Cytotoxicity assay

Cell Counting Kit-8 (DOJINDO, Japan) was used to evaluate the cytotoxic effects of compounds on RAW 264.7 macrophages. Macrophages (3×10^3 cells/well) were seeded in a 96-well cell culture plate and incubated at 37 °C in a 5% CO₂ atmosphere for 2h. After that, the culture medium were removed and adhered cells were exposed to the compounds at 10µM to 1mM for 24h under the same incubation conditions. Each assay was performed in triplicate with independent experiment. Compounds with less cytotoxicity will be used in subsequent experiments.

In vitro assays for anti- *Toxoplasma gondii* activity

Tachyzoites were collected and loaded in triplicate in a 96-well cell culture plate at 5×10^5 cells/per well and challenged with compounds at 1µM and 10µM for 24 h. Parasite survival was performed after stimulation by a standard trypan blue dye exclusion test to determine the number of viable cells. Medium alone was used as control. All of the cultures were performed independent times, and the results are expressed as the percentage of inhibition (I%), which is equal to $[(\text{number of parasites in culture medium} - \text{number of parasites in medium with compounds}) / \text{number of parasites in culture medium}] \times 100\%$.

After that, several compounds with higher inhibition rate were selected. Parasites were collected and loaded as previously described but challenged with the selected compounds at different concentrations ranging from 0 to 200 M for 24 h. The results are expressed as the IC₅₀ (50% inhibitory concentration) values.

In vivo assays for anti- *Toxoplasma gondii* activity

RAW 264.7 macrophages (2×10^5 cells/well) were seeded in a 24-well cell culture plate and incubated at 37 °C in a 5% CO₂ atmosphere with sterile glass for 2h. Cells were infected with RH tachyzoites at a 10:1 parasite-to-cell ratio for 2 h, and after the replacement of the medium with new culture medium, azithromycin, pyrimethamine and compounds at IC₅₀ were added for an extra 36h. Infected and stimulated cells were then observed with an optical microscope and Wright's stain (NJJCBIO, China). The average number of tachyzoites in each cell was determined by randomly counting 200 infected cells in each of the duplicate coverslips.

Ultrastructural analysis by transmission electron microscopy

Approximately 4×10^7 tachyzoites were employed for co-culture with compounds, azithromycin, and pyrimethamine for 18h, and 4×10^7 tachyzoites without any treatment, followed fixed in 3% glutaraldehyde and immediately fixed again at 4°C with 1% osmium tetroxide solution. The samples were thoroughly rinsed with distilled water, and then dehydrated with an acetone gradient, and then transferred to SPI-Pon812 resin for polymerization and embedding. After sectioning, electron staining was performed sequentially with 2% uranyl acetate solution and Reynolds' lead citrate solution. Stained sections were imaged on a Hitachi HT7800 transmission electron microscope.

Phosphatidylserine (PS) exposure and cell death.

Approximately 1×10^6 tachyzoites were treated with compounds, azithromycin, pyrimethamine and the positive control staurosporine for 18h, followed by collection and centrifugation at 1,300 ×g for 15 min at 4°C to remove the supernatants before the addition of annexin V-FITC dye (BD, USA) in the dark for 10 min. After the addition of PI dye for another 5 min followed by the addition of the ligation buffer, the mixture was subjected to flow cytometry (BD, FACS Celesta) or confocal microscopy (Zeiss, LSM880) for further detection, as required by the protocol.

Measurement of changes in mitochondrial membrane potential.

1×10^6 tachyzoites were collected and centrifuged at 1,300 ×g for 15 min at 4°C employed after coculturing with compounds, azithromycin, pyrimethamine and 5µM carbonyl cyanide m-chlorophenylhydrazone (CCCP) (a respiratory uncoupler) for 18h. Then, JC-1 dye were added in the dark and incubate at 37°C for 20 min. After incubation, centrifuge tachyzoites for 15 minutes at 1300× g at 4°C and carefully aspirate the supernatants. Adding staining buffer (1×) to suspend tachyzoites, the mixture was subjected to flow cytometry (BD, FACS Celesta) or confocal microscopy (Zeiss, LSM880) for further detection, as required by the protocol.

Monitoring of changes in intracellular Ca²⁺ levels.

Approximately 1×10^6 tachyzoites were cocultured with compounds, azithromycin, and pyrimethamine for 18h. Next, the tachyzoites were collected and centrifuged followed by incubated (20 min at 37°C) in a cocktail of 5mM Fluo-4 AM, 20% Pluronic F-127 and HBSS (Solarbio, China). Then, 5 times the volume of

HBSS containing 1% fetal bovine serum were added into the mixture followed by incubation at 37°C for 40 min. After incubation, the tachyzoites were washed three times and suspended in HEPES buffer saline. The mixture was subjected to flow cytometry (BD, FACS Celesta) or confocal microscopy (Zeiss, LSM880) for further detection, as required by the protocol.

Invasion Activity

The tachyzoites were collected in 96-well culture plates at a concentration of 1×10^7 cells/well with the addition of compounds, azithromycin, and pyrimethamine. After cocultured at 37 °C in a 5% CO₂ atmosphere for 18h, they were collected and centrifugated at 1,300 ×g for 15 min at 4°C.

The macrophages (2×10^5 cells/well) were seeded in a 24-well cell culture plate and incubated at 37 °C in a 5% CO₂ atmosphere with sterile glass for 2h. The cells were infected with the tachyzoites that collected before at a 10:1 parasite-to-cell ratio for 4 h. Infected and stimulated cells were then observed with an optical microscope and Wright's stain. The average number of tachyzoites in each cell was determined by randomly counting 200 infected cells in each of the duplicate coverslips.

Macrophage phagocytosis

Macrophages (1×10^5 cells/well) were cultured for 24 h in the presence of the following compounds, azithromycin, and pyrimethamine. Cells were washed by PBS and incubated with 50µg/ml zymosan (Solarbio, China) in new medium for 3h incubation. Cells were then observed with an optical microscope and Wright's stain. The average number of zymosan granules in each cell was determined by randomly counting 200 infected cells in each of the duplicate coverslips.

Lysosomal Activity.

Macrophages (1×10^5 cells/well) were plated and incubated with compounds, azithromycin, and pyrimethamine for 24 h. After the replacement of the medium, 20µL of neutral red solution (Beyotime, China) was added and incubated for 2h. After that, the supernatant was discarded, the cells were washed with PBS, and 200µl of Neutral Red Detection Lysis Solution (Beyotime, China) was added. After 10 min on a shaker (QILINBEIER, TS-1), the plate was read at 540 nm by using an ELISA plate reader (TECAN, Sunrise-basic).

Statistics.

IC₅₀ was calculated according to a nonlinear regression using a log inhibitor-versus-response equation with 95% confidence intervals by GraphPad Prism (version 8.0) software. The data were analyzed by Student's t test for comparison of two groups or by one-way analysis of variance (ANOVA) for comparison of three or more groups using GraphPad Prism (version 8.0) software. Significant differences were determined and designated with asterisks as follows: *P < 0.05; **P < 0.01; ***P < 0.001 and ****P < 0.0001.

Result

Preliminary selecting of compounds.

We first examined the cytotoxicity effects of compounds against macrophage at two different concentrations (1 μ M and 10 μ M) by directly adding compounds into cells for 24 h. The results showed that only a few of the compounds had high cytotoxicity (data did not show). Secondly, we examined the inhibitory effects of the compounds with low cytotoxicity against RH tachyzoites at the concentrations of 1 μ M and 10 μ M by directly adding them into the extracellular cultivation system of tachyzoites for 24 h. Seven compounds were screened out following a standard of high inhibitory rates and low cytotoxicity from 36 compounds (Table 1.). In addition, the cytotoxicity effects of the positive control, pyrimethamine, against macrophage and RH tachyzoites were also examined.

Anti-tachyzoite activity and cytotoxicity assay

Selected compounds were added directly to the extracellular culture system of tachyzoites and to macrophages, respectively, and incubated for 24 h at concentrations ranging from 50nM to 20 μ M. The results showed a significant concentration-dependent increase in parasite inhibitory (Fig 1). It could be seen that when the concentration was greater than or equal to 10 μ M, the inhibition rate of *T. gondii* could reach the highest value. However, the inhibition rate of each compound at low concentration was not the same. At low concentrations, the inhibitory effect of HZS-2079B on *T. gondii* was not ideal. Instead, YCC-10-105 and YCC-13-175 still had high inhibition rate at low concentrations. And the trend of the inhibition rate curve was similar to that of the clinical medication azithromycin. The IC₅₀ and CC₅₀(50% cytotoxic concentration) of each compound were showed in Table 2. And the IC₅₀ of pyrimethamine was 17.78 μ M based on the previous experiments' data. The results showed that pyrimethamine and azithromycin were more effective in inhibiting tachyzoite in vitro than those compounds, but the safety of which was lower than that of them based on the cytotoxicity. Therefore, considering the anti-tachyzoite activity and cytotoxicity, YCC-10-151-P1 and YCC-10-174 were selected as ideal compounds for subsequent experiments. Moreover, the subsequent administration concentration of YCC-10-151-P1, YCC-10-174, pyrimethamine and azithromycin was about their IC₅₀ value, which were 500nM, 650nM, 20 μ M, and 60nM, respectively.

Ultrastructural structure of tachyzoites.

We observed the changes in the ultrastructure of the tachyzoites treated with YCC-10-151-P1 and YCC-10-174 through a transmission electron microscope (Fig 2). Some of the untreated tachyzoites died after 18h in culture cells. However, most of the morphology remained crescent-shaped, with slight changes in the structure of intracellular organelles. After 18h of treatment with pyrimethamine and azithromycin, most of the tachyzoites died, with incomplete and fragmented morphology. The rest of the tachyzoites that were still alive had increased vacuoles and swelling of mitochondria, indicating a possibility of necrosis. In addition, the changes in the nucleus were also been observed. Compared with the control group, the perinuclear space of the tachyzoites in the experimental groups was obviously widened, and

the nuclear membrane was also thickened. Nuclear pyknosis and increased heterochromatin could also be observed.

Cell death of tachyzoites.

To determine whether the death of tachyzoites triggered by YCC-10-151-P1 and YCC-10-174 involved apoptosis, we evaluated the exposure of phosphatidylserine, a marker of the initiation of the early apoptotic process. RH tachyzoites were treated with YCC-10-151-P1 and YCC-10-174 for 18 h, followed by PS detection through annexin V-fluorescein isothiocyanate (FITC) labeling. Compounds-treated tachyzoites showed visible red fluorescence compared to the control group when the tachyzoites were examined under a confocal microscope (Fig. 3A). The average ratio of red and green fluorescence intensity of the tachyzoites in each group was determined by randomly analyzing 100 tachyzoites (Fig. 3B). It was indicated that untreated tachyzoites cultured in medium had a certain degree of apoptosis and the process of apoptosis had been accelerated by both compounds treatment and the positive control. Furthermore, when subjected to flow cytometry for further counting, both the early apoptotic mortality and the total mortality (include early and late apoptotic/necrotic) ratio for the compounds-treated groups were significantly different from that for the positive control treated group (Fig. 3C), same as the results we obtained under the confocal microscope. In addition, pyrimethamine and azithromycin as traditional therapeutic drugs and the positive control staurosporine (50 μ M) also induced a substantial increase in cell death and apoptosis, although the average ratio of red and green fluorescence intensity of pyrimethamine-treated tachyzoites only slightly increased.

Mitochondrion depolarization in tachyzoites.

Mitochondria is the organelle that plays an important role in energy metabolism, and the dysfunction of this organelle has been reported to be one of the reasons for the death of parasites[16]. The decrease of mitochondrial membrane potential was a signature event in the stage of classical apoptosis initiated from mitochondria. Therefore, we examined mitochondrial membrane potential ($\Delta\Psi_m$) to explore whether it is the pathway by which compounds trigger apoptosis. The RH tachyzoites were stimulated with YCC-10-151-P1, YCC-10-174, pyrimethamine and azithromycin and CCCP (5 μ M) as the reference compound for 18h. Confocal microscopy was used to visualize depolarization, along with flow cytometry to quantitate $\Delta\Psi_m$. Microscopic observations (Fig. 4A) revealed that the tachyzoites treated with two compounds, YCC-10-151-P1 and YCC-10-174, exhibited significantly greater fluorescence in the green region than the red region. The pyrimethamine-treated group, azithromycin-treated group and the positive group were also observed the similar results as those two compounds-treated groups, indicating a decreased $\Delta\Psi_m$. On the contrary, significantly greater fluorescence in the red region than the fluorescence in the green region was observed in the control group, indicating an increased $\Delta\Psi_m$. The result of the JC-1 fluorescence intensity ratio (red/green) was shown in Fig. 4B. Both compounds and drugs treatments resulted in a decreased ratio by 5 to 10 times. Flow cytometric analysis of the YCC-10-151-P1-treated and YCC-10-174-treated tachyzoites showed 34.9% and 40.7% depolarized mitochondria, compared to

untreated tachyzoites 9.04% (Fig. 4C), which was similar to the trend we observed under the confocal microscope.

Elevation of cytosolic calcium levels.

Disruption of calcium homeostasis resulting from the release of intracellular stores of calcium was a key event triggered by chemotherapeutic agents[17, 18], and there was a strong link between changes in calcium homeostasis and the collapse of mitochondrial membrane potential[19]. The intracellular calcium level could be measured by using the dye Fluo-4 AM. After cocultured with YCC-10-151-P1, YCC-10-174, pyrimethamine and azithromycin and CCCP for 18h, the RH tachyzoites showed great fluorescence under the confocal microscope, especially the CCCP-treated tachyzoites. In contrast, fluorescence could barely be seen in the untreated tachyzoites (Fig. 5A). Compared with the control group, the fluorescence intensity of in the other groups increased nearly 2~4 fold (Fig. 5B).

Inhibition of invasion activity and intracellular growth

We further assessed whether these compounds affected the ability of RH tachyzoites to invade cells. RH tachyzoites were stimulated with YCC-10-151-P1 and YCC-10-174 for 18h, followed by infection of mouse RAW 264.7 macrophages for 4h. By counting the number of tachyzoites in each infected cell, we demonstrated that the invasion ability of tachyzoites treated with YCC-10-151-P1 and YCC-10-174 was reduced (Fig. 6), particularly the YCC-10-174-treated group, similar to the results obtained for the pyrimethamine and azithromycin groups.

Then, the effect of YCC-10-151-P1 and YCC-10-174 on the growth of intracellular tachyzoites was evaluated. First, a RAW 264.7 mouse macrophage infection model with a parasite/host cell ratio of 10:1 was constructed, followed by challenge with YCC-10-151-P1 and YCC-10-174 for 36h. By counting the number of tachyzoites in each infected cell, it was observed that the average number of tachyzoites in macrophages in the negative control group was about 14, while the average number of intracellular tachyzoites was significantly decreased after treatment. Among them, the YCC-10-174 treatment group and the pyrimethamine treatment group had the most significant decline, which were about 9 tachyzoites/cell and 7 tachyzoites/cell, respectively. The average number of tachyzoites in YCC-10-151-P1-treated group and azithromycin-treated group were about 9.8/cell and 10.6/cell, respectively. It could demonstrate that macrophages stimulated with both YCC-10-151-P1 and YCC-10-174 had the ability to kill the intracellular parasites (Fig. 7), similar to the result obtained for the pyrimethamine and azithromycin treated groups.

Lysosomal Activity and Phagocytosis Assay

After we obtained the results, we had an interest to pursue the possibility that the two target compounds achieved this effect by activating macrophages for defense. Phagocytosis and the lysosomal system are critical to macrophage function due to their role in host defense. Hence, we evaluated the lysosomal activity and phagocytic activity of cells by two indicators: the absorbance of neutral red and the number

of intracellular zymosan A particles. Lysosomal activity of macrophage was evaluated based on the retention of neutral red in lysosomes and determined by colorimetry. Compared to untreated-control group, The lysosomal activity of macrophages treated with YCC-10-174 showed a statistically significant increase while the YCC-10-151-P1 and azithromycin-treated groups increased only on a minor scale (Fig.8A). However, macrophage cocultured with pyrimethamine were observed to have a statistically significant decrease in lysosomal activity.

Macrophage phagocytosis was reflected by the phagocytosis of zymosan A after drug stimulation. By counting the number of zymosan A particles in each stimulated cell, there was a significant increase both in YCC-10-151-P1, YCC-10-174 and pyrimethamine group (Fig.8 B.C). In addition, azithromycin stimulated macrophage were observed to have an increase in the number of zymosan A particles, but that was not significantly different from control group.

Discussion

There were many species of *Chloranthecae* spp., which were widely used in China. Based on pharmacological knowledge, studies had confirmed that *Chloranthecae* spp. had great biological activity and could be used for the treatment of tumors, infectious fungi or viruses[20, 21, 22, 23]. A recent article reported that *chlorajaponilide C* was very potent against *Plasmodium falciparum in vitro*. [24] Therefore, we focused on the small molecule intermediate products of terpenoid natural product, *chlorajaponilide C*, characterizing the anti-toxoplasma property by evaluating the killing effects of those compounds upon extracellular and intracellular tachyzoites of the RH strain of *T. gondii*. In this experiment, 36 compounds were initially screened. The purpose was to screen out compounds with high rates of inhibition activity of *T. gondii* but low cytotoxicity of cells. YCC-10-151-P1, YCC-10-174 and YCC-13-175 were the best among all compounds, with lower IC₅₀ on tachyzoites and higher CC₅₀ on macrophages. Unfortunately, the inhibitory effect of YCC-13-175 was not ideal in intracellular experiments. The average number of tachyzoites in macrophages in the negative control group was about 10.59, while the average number of tachyzoites in the YCC-13-175 treatment group was about 9.41, with only a slight decrease. Therefore, YCC-10-151-P1 and YCC-10-174 were finally selected for subsequent experiments.

In order to clarify the mechanism by which YCC-10-151-P1 and YCC-10-174 act against RH tachyzoites, we carried out a series of experiments to evaluate the proliferation and death of the parasites. To observe early apoptotic and mid-to-late apoptotic/necrotic signals, we shortened the incubation time from 24 h to 18 h. As we have seen, tachyzoites would undergo a certain degree of apoptosis even without any treatment for 18 h *in vitro*, because *T. gondii* is an obligate intracellular parasite. The co-cultivation with the compounds greatly promoted the process of tachyzoite apoptosis. Compared with the control group, treatment with two compounds and two clinical treatment drugs would increase the proportion of early apoptosis, while staurosporine, a typical pro-apoptosis inducer, mainly led to an increase in the proportion of late apoptosis. Aloui Z et al. treated *leishmania* promastigotes for 24h and 72h with two essential oils containing oxidized monoterpenes and monoterpene hydrocarbons extracted from *Artemisia campestris* and *Artemisia herba-alba* plants, respectively, and both essential oils were found to

trigger early apoptosis in a dose- and time-dependent manner while still remaining cell membranes intact [25]. This was consistent with the trend of our results. They further analyzed the cell cycle and found that there was cell cycle arrest in sub-G0/G1 phase. Some other natural or synthetic substances containing terpenoids, such as artemisinin [26], oxoallobetulin [27], *Artemisia annua* leaf essential oil [28], also had similar anti-*leishmania* effects. Terpenoid-induced cell cycle arrest might be a mechanism leading to parasite apoptosis.

For protozoa such as *T. gondii* and *Leishmania*, the main source of energy is mitochondria. The mitochondrial membrane potential ($\Delta\Psi_m$) is essential for normal cell function and maintenance of cell viability. Therefore, mitochondrial dysfunction led to depolarization of $\Delta\Psi_m$ and even cell death [29]. As an early event of apoptosis, the change of $\Delta\Psi_m$ was hyperpolarized, and the subsequent decrease of $\Delta\Psi_m$ was a typical late event of apoptosis [30]. After observing that compound treatment promoted apoptosis of tachyzoites and mitochondrial swelling under TEM, we further examined changes in $\Delta\Psi_m$ of treated tachyzoites, using the respiratory decoupler CCCP as a positive control. Consistent with our expected results, a decrease in $\Delta\Psi_m$ was observed in the treated tachyzoites in contrast to the untreated tachyzoites, with a larger decrease caused by YCC-10-174 and pyrimethamine. Myrislignan, a natural product from *Myristica fragrans* Houtt, had potent inhibition of *T. gondii* *in vitro* and *in vivo*. In tachyzoites treated with Myrislignan for 8 h, significant mitochondrial damage was observed under both electron microscopy and flow cytometry, suggesting that anti-*T. gondii* activity of Myrislignan was related to its interference with *T. gondii* mitochondrial function [31]. Yamamoto ES et al. demonstrated that Ursolic acid triggered an early programmed cell death events which was associated with the hyperpolarized state of mitochondria [32]. Therefore, we believed that YCC-10-151-P1 and YCC-10-174 promoted the apoptosis process of *T. gondii* by triggering a mitochondrial hyperpolarized state. Therefore, mitochondrial membrane potential was elevated as untreated tachyzoites were in the early apoptotic stage. YCC-10-151-P1 and YCC-10-174 showed mitochondrial depolarization due to the promotion of tachyzoite apoptotic process.

Dysfunction of mitochondrial function could also lead to a series of changes in metabolism and homeostasis, including effects on the dynamic regulation of Ca^{2+} [33]. Calcium metabolism is very important for apicomplexan parasites because calcium is involved in several important functions of apicomplexan parasite invasion, motility and differentiation [34]. Calcium overload due to increased mitochondrial Ca^{2+} uptake can triggered *T. cruzi* cell death [35]. After observing mitochondria damage, we used Fluo-4 A, M staining to detect whether the Ca^{2+} concentration in the tachyzoites would change. Stimulation of YCC-10-151-P1 and YCC-10-174 resulted in an increase in the fluorescence intensity of the dye even exceeding the concentration increase caused by treatment with the positive control CCCP, indicating an increase in cytoplasmic calcium storage. Miltefosine, an approved anti-*Leishmania* drug, had mechanisms of action including induction of increased intracellular Ca^{2+} levels and mitochondrial depolarization [36]. Other terpenoids also induced an increase in Ca^{2+} concentration in the parasites [37, 38]. Therefore, we speculated that the increase of calcium ion concentration in tachyzoites caused by the two target compounds might be related to their effects on mitochondrial. In addition to directly interacting

with calcium pumps to regulate calcium homeostasis, terpenoids might cause changes in parasite calcium concentrations through other means of regulating calcium transport across membranes [39, 40]

Next, we evaluated the effect of compound treatment on the ability of tachyzoites to invade cells. Macrophages were infected with tachyzoites treated with compounds and drugs for 18 h, and it was found that the ability of the treated tachyzoites to invade cells was significantly reduced. Based on the previous results, we believed that the inhibition of YCC-10-151-P1 and YCC-10-174 led to the impairment of the normal physiological function of tachyzoites and the decreased invasive ability.

We wondered whether YCC-10-151-P1 and YCC-10-174 also had inhibitory effects on tachyzoites in cells, after evaluating their direct inhibitory effect on tachyzoites *in vitro*. Macrophages are an important part of the immune system and play a very important role in eliminating pathogens. And because macrophages are nucleated cells, the invasion of tachyzoites is both active and passive. We assessed the effect of YCC-10-151-P1 and YCC-10-174 on intracellular tachyzoite growth by constructing a RAW 264.7 mouse macrophage infection model, followed by the addition of these two compounds and incubation for 36 h. The results showed that both YCC-10-151-P1 and YCC-10-174 effectively reduced the number of tachyzoites in cells. Phagocytosis and the lysosomal system are required for antigen internalization, degradation, and presentation, so they are particularly important for macrophage function. We therefore assessed whether targeted compounds affected the function of macrophages to eliminate intracellular tachyzoites. Surprisingly, phagocytosis was upregulated in macrophages co-cultured with both YCC-10-151-P1 and YCC-10-174 for 24 h, whereas only YCC-10-174 treatment upregulated lysosomal activity in macrophages. Azithromycin did not significantly increase lysosomal activity or phagocytosis of macrophages. In contrast, pyrimethamine increased the phagocytic activity of macrophages but decreased lysosomal activity. Rodrigues KA and colleagues found that sesquiterpene-rich *Eugenia uniflora* L. essential oil (EuEO), extracted from the Brazilian cherry tree, activated macrophages through an increase in phagocytic capacity and lysosomal activity [41]. *Myracrodruon urundeuva* essential oil (MuEO), rich in monoterpenoids, induced enhanced macrophage phagocytosis but had no effect on lysosomal activity [42]. Activation of macrophages by increasing nitric oxide (NO) was a major mechanism of protective immunity against *Leishmania* [43]. Other studies had shown that some terpenoids activated macrophages by mediating the production of NO by macrophages, thereby killing intracellular parasites [44, 45]. However, the activation of macrophages by EuEO and MuEO was not mediated by increased NO production. The possible reason for this might be that terpenoids could achieve additional antiparasitic activity through different mechanisms affecting the host immune system.

•

Conclusions

In summary, the small molecular intermediate products of chlorajaponilide C, a natural product of terpenoids extracted from *Chloranthaceae* spp, were able to inhibit the growth of RH tachyzoites both *in*

vivo and vitro. They accelerated the apoptotic process of tachyzoites by causing depolarization of mitochondria, influx of Ca^{2+} and altering lipid metabolism. At the same time, they also interacted with the host's immune system to promote the inhibition of parasites. The most important thing was that they had low cytotoxicity. Therefore, they could be further modified and expected to become new anti-parasitic clinical drugs.

Abbreviations

IC_{50}

50% inhibitory concentration

CC_{50}

50% cytotoxic concentration

Declarations

Acknowledgments.

Not applicable.

Authors' contributions

QWC, ZYJ, KD and JPC designed and supervised the study. ZYJ, DK, ZSH and CCY undertook the laboratory work. ZYJ and KD wrote the manuscript. QWC, BL and JPC revised the manuscript and polished the language. All authors read and approved the final manuscript.

Funding

This work was supported by the National Natural Science Foundation of China (grant numbers 8190081387,81672048).

Availability of data and materials

The datasets supporting the conclusions of this article are included within the article.

Competing interests

We declare that we have no competing interests.

References

1. Hide G. Role of vertical transmission of *Toxoplasma gondii* in prevalence of infection. Expert review of anti-infective therapy. 2016;14 3:335-44.

2. Almeria S, Dubey JP. Foodborne transmission of *Toxoplasma gondii* infection in the last decade. An overview. *Research in veterinary science*. 2021;135:371-85.
3. Mcleod R, Cohen W, Dovgin S, Finkelstein L, Boyer KM. Human *Toxoplasma* infection - ScienceDirect. 2020.
4. Rostami A, Riahi SM, Gamble HR, Fakhri Y, Gasser RB. Global prevalence of latent toxoplasmosis in pregnant women: a systematic review and meta-analysis. *Clinical Microbiology and Infection*. 2020;26 6.
5. Florence RG, Valeria M, Damien D, Fran?oise B, Aguado GJM, Marie-Pierre BP, et al. Toxoplasmosis in Transplant Recipients, Europe, 2010-2014. *Emerging Infectious Diseases*. 2018;24 8:1497-504.
6. Robert-Gangneux F, Darde ML. Epidemiology of and diagnostic strategies for toxoplasmosis. *Clin Microbiol Rev*. 2012;25 2:264-96.
7. Foppa. Toxoplasmosis of the Central Nervous System in the Acquired Immunodeficiency Syndrome – NEJM. *Lancet*. 1992.
8. Deng Y, Wu T, Zhai S-Q, Li C-H. Recent progress on anti-*Toxoplasma* drugs discovery: Design, synthesis and screening. *European Journal of Medicinal Chemistry*. 2019;183:111711.
9. Wang JL, Zhang NZ, Li TT, He J, Elsheikha HM, Zhu XQ. Advances in the Development of Anti-*Toxoplasma gondii* Vaccines: Challenges, Opportunities, and Perspectives. *Trends in Parasitology*. 2019.
10. Montazeri M, Mehrzadi S, Sharif M, Sarvi S, Shahdin S, Daryani A. Activities of anti-*Toxoplasma* drugs and compounds against tissue cysts in the last three decades (1987 to 2017), a systematic review. *Parasitology Research*. 2018;117 10:3045-57.
11. Sepulveda-Arias JC, Veloza LA, Mantilla-Muriel LE. Anti-*Toxoplasma* activity of natural products: a review. *Recent patents on anti-infective drug discovery*. 2014;9 3:186-94.
12. Mirzaalizadeh B, Sharif M, Daryani A, Ebrahimzadeh MA, Zargari M, Sarvi S, et al. Effects of *Aloe vera* and *Eucalyptus* methanolic extracts on experimental toxoplasmosis in vitro and in vivo. *Exp Parasitol*. 2018;192:6-11.
13. Zhang LH, Jin LL, Liu F, Jin C, Wei ZY. Evaluation of ursolic acid derivatives with potential anti-*Toxoplasma gondii* activity. *Experimental Parasitology*. 2020;216:107935.
14. Darne P, Escotte-Binet S, Cordonnier J, Remy S, Hubert J, Sayagh C, et al. Anti-*Toxoplasma gondii* effect of lupane-type triterpenes from the bark of black alder (*Alnus glutinosa*) and identification of a potential target by reverse docking. *Parasite (Paris, France)*. 2022;29:7.
15. Yuan C, Deng BDH, Man Y, Liu B. Total Syntheses of Sarcandrolide J and Shizukaol D: Lindenane Sesquiterpenoid 4+ 2 Dimers (vol 56, pg 637, 2017). *Angewandte Chemie-International Edition*. 2022;61 2.
16. Wang H, Li C, Ye W, Pan Z, Sun J, Deng M, et al. *Toxoplasma gondii* Induces Apoptosis via Endoplasmic Reticulum Stress-Derived Mitochondrial Pathway in Human Small Intestinal Epithelial Cell-Line. *The Korean journal of parasitology*. 2021;59 6:573-83.

17. Dolai S, Pal S, Yadav RK, Adak S. Endoplasmic reticulum stress-induced apoptosis in *Leishmania* through Ca²⁺-dependent and caspase-independent mechanism. *The Journal of biological chemistry*. 2011;286 15:13638-46.
18. de Macedo-Silva ST, de Oliveira Silva TL, Urbina JA, de Souza W, Rodrigues JC. Antiproliferative, Ultrastructural, and Physiological Effects of Amiodarone on Promastigote and Amastigote Forms of *Leishmania amazonensis*. *Molecular biology international*. 2011;2011:876021.
19. Mukherjee SB, Das M, Sudhandiran G, Shaha C. Increase in cytosolic Ca²⁺ levels through the activation of non-selective cation channels induced by oxidative stress causes mitochondrial depolarization leading to apoptosis-like death in *Leishmania donovani* promastigotes. *The Journal of biological chemistry*. 2002;277 27:24717-27;
20. Xu YJ, Tang CP, Ke CQ, Zhang JB, Weiss HC, Gesing ER, et al. Mono- and Di-sesquiterpenoids from *Chloranthus spicatus*. *J Nat Prod*. 2007;70 12:1987-90;
21. Zhang M, Wang JS, Wang PR, Oyama M, Luo J, Ito T, et al. Sesquiterpenes from the aerial part of *Chloranthus japonicus* and their cytotoxicities. *Fitoterapia*. 2012;83 8:1604-9;
22. Fang PL, Cao YL, Yan H, Pan LL, Liu SC, Gong NB, et al. Lindenane disesquiterpenoids with anti-HIV-1 activity from *Chloranthus japonicus*. *J Nat Prod*. 2011;74 6:1408-13.
23. Guo YQ, Tang GH, Li ZZ, Lin SL, Yin S. Chlojapolactone A, An Unprecedented 1,3-Dioxolane Linked-Lindenane Sesquiterpenoid Dimer from *Chloranthus japonicus*. *RSC Advances*. 2015;5 125:103047-51.
24. Butler JH, Baptista RP, Valenciano AL, Zhou B, Kissinger JC, Tumwebaze PK, et al. Resistance to Some But Not Other Dimeric Lindenane Sesquiterpenoid Esters Is Mediated by Mutations in a *Plasmodium falciparum* Esterase. *ACS infectious diseases*. 2020;6 11:2994-3003;
25. Aloui Z, Messaoud C, Haoues M, Neffati N, Bassoumi Jamoussi I, Essafi-Benkhadir K, et al. Asteraceae *Artemisia campestris* and *Artemisia herba-alba* Essential Oils Trigger Apoptosis and Cell Cycle Arrest in *Leishmania infantum* Promastigotes. *Evidence-based complementary and alternative medicine : eCAM*. 2016;2016:9147096;
26. Sen R, Bandyopadhyay S, Dutta A, Mandal G, Ganguly S, Saha P, et al. Artemisinin triggers induction of cell-cycle arrest and apoptosis in *Leishmania donovani* promastigotes. *Journal of medical microbiology*. 2007;56 Pt 9:1213-8;
27. Ghosh P, Mandal A, Dey S, Pal C. Synthesis and in vitro Screening of 29, 30-Dibromo-28-oxoallobetulin against Parasitic Protozoans, *Leishmania donovani* and *Leishmania Major*. *Indian journal of pharmaceutical sciences*. 2015;77 2:202-7.
28. Islamuddin M, Chouhan G, Want MY, Tyagi M, Abdin MZ, Sahal D, et al. Corrigendum: Leishmanicidal activities of *Artemisia annua* leaf essential oil against Visceral Leishmaniasis. *Front Microbiol*. 2015;6:1015.
29. Zorova LD, Popkov VA, Plotnikov EY, Silachev DN, Pevzner IB, Jankauskas SS, et al. Mitochondrial membrane potential. *Analytical Biochemistry*. 2018;552:50-9; doi:

30. Giovannini C, Matarrese P, Scazzocchio B, Sanchez M, Masella R, Malorni W. Mitochondria hyperpolarization is an early event in oxidized low-density lipoprotein-induced apoptosis in Caco-2 intestinal cells. *FEBS letters*. 2002;523 1-3:200-6.
31. Zhang J, Si H, Li B, Zhou X, Zhang J. Myrislignan Exhibits Activities Against *Toxoplasma gondii* RH Strain by Triggering Mitochondrial Dysfunction. *Front Microbiol*. 2019;10:2152.
32. Yamamoto ES, Campos BL, Jesus JA, Laurenti MD, Ribeiro SP, Kallás EG, et al. The Effect of Ursolic Acid on *Leishmania (Leishmania) amazonensis* Is Related to Programed Cell Death and Presents Therapeutic Potential in Experimental Cutaneous Leishmaniasis. *PLoS One*. 2015;10 12:e0144946.
33. Marchi S, Patergnani S, Missiroli S, Morciano G, Rimessi A, Wieckowski MR, et al. Mitochondrial and endoplasmic reticulum calcium homeostasis and cell death. *Cell Calcium*. 2018;69:62-72;
34. Moreno SNJ, Ayong L, Pace DA. Calcium storage and function in apicomplexan parasites. *Essays Biochem*. 2011;51:97-110.
35. Duchen MR. Mitochondria and calcium: from cell signalling to cell death. *The Journal of physiology*. 2000;529 Pt 1 Pt 1:57-68.
36. Pinto-Martinez AK, Rodriguez-Durán J, Serrano-Martin X, Hernandez-Rodriguez V, Benaim G. Mechanism of Action of Miltefosine on *Leishmania donovani* Involves the Impairment of Acidocalcisome Function and the Activation of the Sphingosine-Dependent Plasma Membrane Ca²⁺ Channel. *Antimicrobial Agents & Chemotherapy*. 2017:1116-9.
37. Londero VS, Costa-Silva TA, Antar GM, Baitello JB, Lago J. Antitrypanosomal Lactones from *Nectandra barbellata*. *Journal of Natural Products*. 2021.
38. Silva GNS, Schuck DC, Cruz LN, Moraes MS, Nakabashi M, Gosmann G, et al. Investigation of antimalarial activity, cytotoxicity and action mechanism of piperazine derivatives of betulinic acid. *Tropical Medicine & International Health*. 2015;20 1:29-39.
39. Isah MB. Terpenoids as Emerging Therapeutic Agents: Cellular Targets and Mechanisms of Action against Protozoan Parasites. *Studies in Natural Products Chemistry*. 2019:227-50.
40. Diedrich D, Wildner AC, Silveira TF, Silva GNS, Santos FD, da Silva EF, et al. SERCA plays a crucial role in the toxicity of a betulinic acid derivative with potential antimalarial activity. *Chemico-biological interactions*. 2018;287:70-7.
41. Rodrigues KA, Amorim LV, de Oliveira JM, Dias CN, Moraes DF, Andrade EH, et al. *Eugenia uniflora* L. Essential Oil as a Potential Anti-*Leishmania* Agent: Effects on *Leishmania amazonensis* and Possible Mechanisms of Action. *Evidence-based complementary and alternative medicine : eCAM*. 2013;2013:279726.
42. Carvalho CE, Sobrinho-Junior EP, Brito LM, Nicolau LA, Carvalho TP, Moura AK, et al. Anti-*Leishmania* activity of essential oil of *Myracrodruon urundeuva* (Engl.) Fr. All.: Composition, cytotoxicity and possible mechanisms of action. *Exp Parasitol*. 2017;175:59-67.
43. Laurenti MD, Passero LF, Tomokane TY, Franceschini Fde C, Rocha MC, Gomes CM, et al. Dynamic of the cellular immune response at the dermal site of *Leishmania (L.) amazonensis* and *Leishmania*

(V.) *braziliensis* infection in *Sapajus apella* primate. *BioMed research international*. 2014;2014:134236.

44. Miranda MM, Panis C, da Silva SS, Macri JA, Kawakami NY, Hayashida TH, et al. Kaurenoic Acid Possesses Leishmanicidal Activity by Triggering a NLRP12/IL-1 β /cNOS/NO Pathway. *Mediators of inflammation*. 2015;2015:392918.
45. Kumar BS, Joydeep P, Kshudiram N, Subir K, Tripti D. Asiaticoside induces tumour-necrosis-factor- α -mediated nitric oxide production to cure experimental visceral leishmaniasis caused by antimony-susceptible and -resistant *Leishmania donovani* strains. *Journal of Antimicrobial Chemotherapy*. 2012; 4:910-20.

Tables

Table 1. Inhibition rates of compounds, azithromycin, and pyrimethamine against tachyzoites of *T. gondii* and macrophages

Compounds	Macrophage inhibition rates (%)		RH tachyzoites inhibition rates (%)	
	Concentrations (10 μ M)	Concentrations (1 μ M)	Concentrations (10 μ M)	Concentrations (1 μ M)
HZS-2039	31.72	0	77.51	60.64
HZS-2079B	0	0	94.34	41.51
DB-17220	0	0	74.53	56.6
YCC-10-151-P1	0	0	97.65	62.44
YCC-10-174	0	0	98.08	51.17
YCC-10-105	0	0	98.18	48.36
YCC-13-175	0	0	98.36	43.66
azithromycin	14.47	5.77	100.00	94.33
pyrimethamine	0	0	93.62	87.94

Table 2. Activity of compounds, azithromycin and against pyrimethamine Tachyzoites of *T. gondii* and Macrophages

Compounds	IC ₅₀ (μM)	CC ₅₀ (μM)
HZS-2039	0.9932	>20
HZS-2079B	7.685	31.86
DB-17220	0.5913	24.26
YCC-10-151-P1	0.4242	1677
YCC-10-174	0.6538	318.8
YCC-13-175	0.08461	757.8
YCC-10-105	0.07976	28.2
azithromycin	0.05691	14.86
pyrimethamine	17.78	402.3

Abbreviations: IC₅₀, 50% inhibitory concentration; CC₅₀, 50% cytotoxic concentration.

Figures

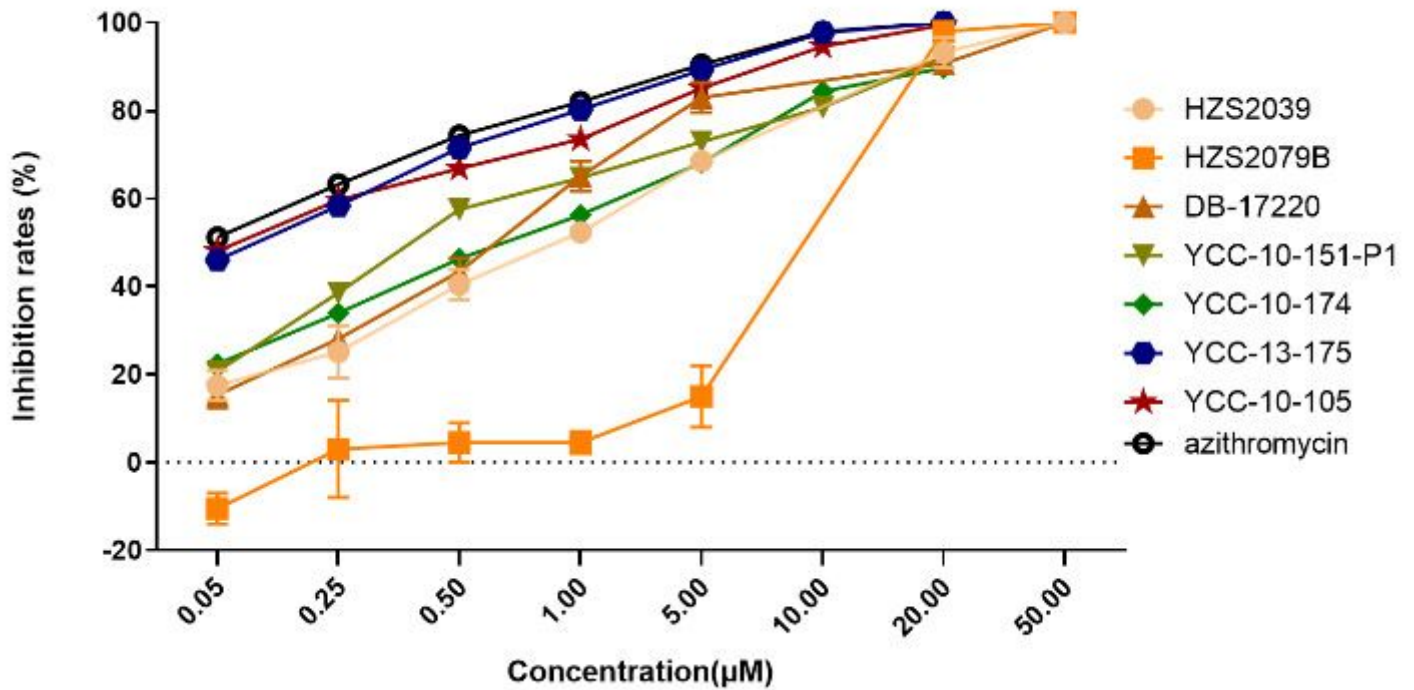


Figure 1

Rates of inhibition of RH tachyzoites by different stimuli. The results are shown as the means \pm standard error of the mean from eight independent experiments.

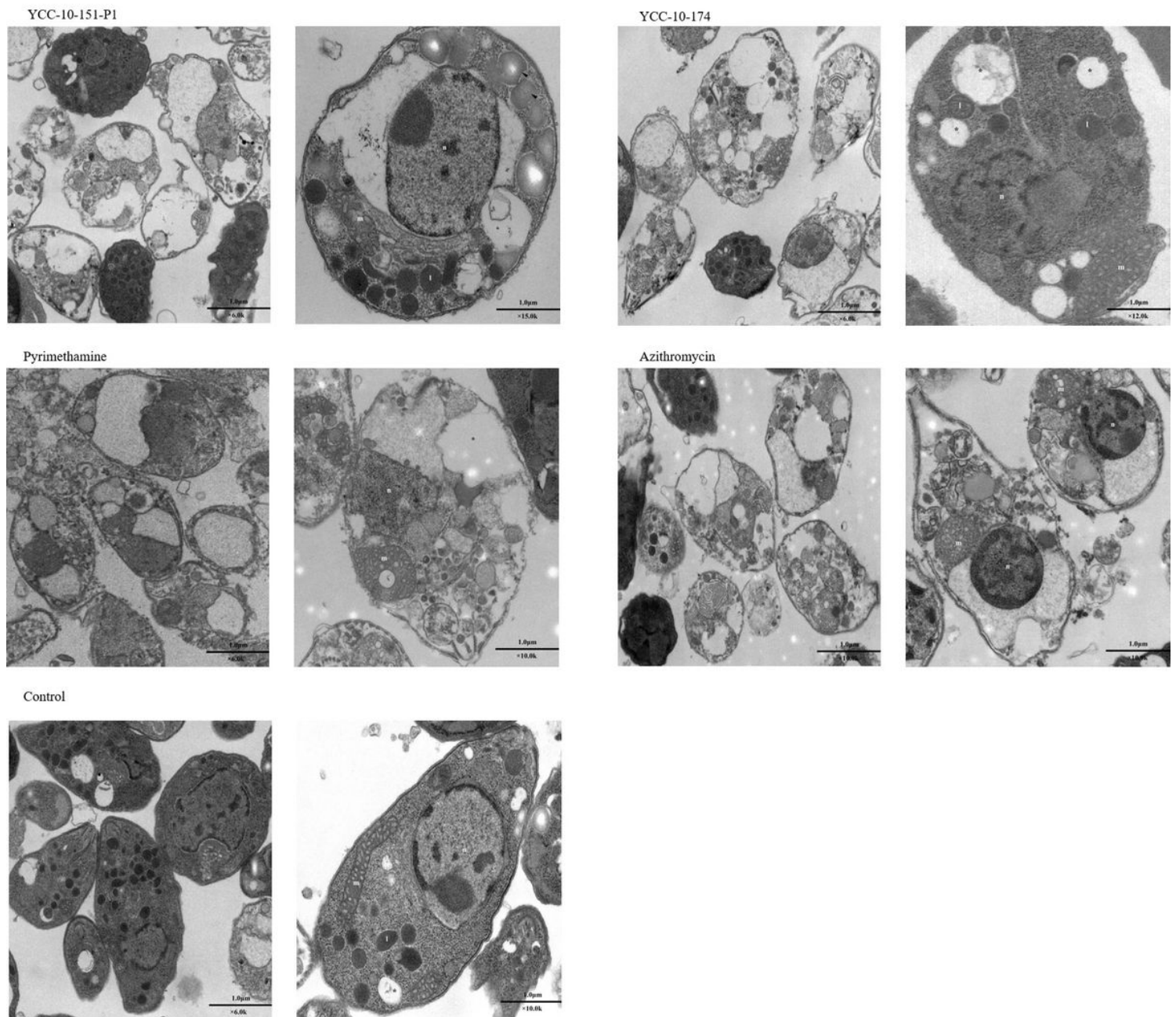


Figure 2

Ultrastructural alterations in tachyzoites. Most of the untreated tachyzoites remained crescent-shaped, with slight changes in the structure of intracellular organelles. In the stimulated tachyzoites, the cell membrane was discontinuous or even ruptured. Larger vacuoles appeared in the cells, and the cell morphology also changed to varying degrees. Changes such as nuclear pyknosis, nuclear membrane thickening, and widening of the perinuclear space could be observed. Mitochondria was also altered by stimulation, mainly necrosis and swelling. In addition, the appearance of lipid reservoirs has been

observed in some tachyzoites. Abbreviations: m, mitochondrial. n, nucleus. l, lysosome. *, vacuoles. Arrowhead, lipid reservoirs.

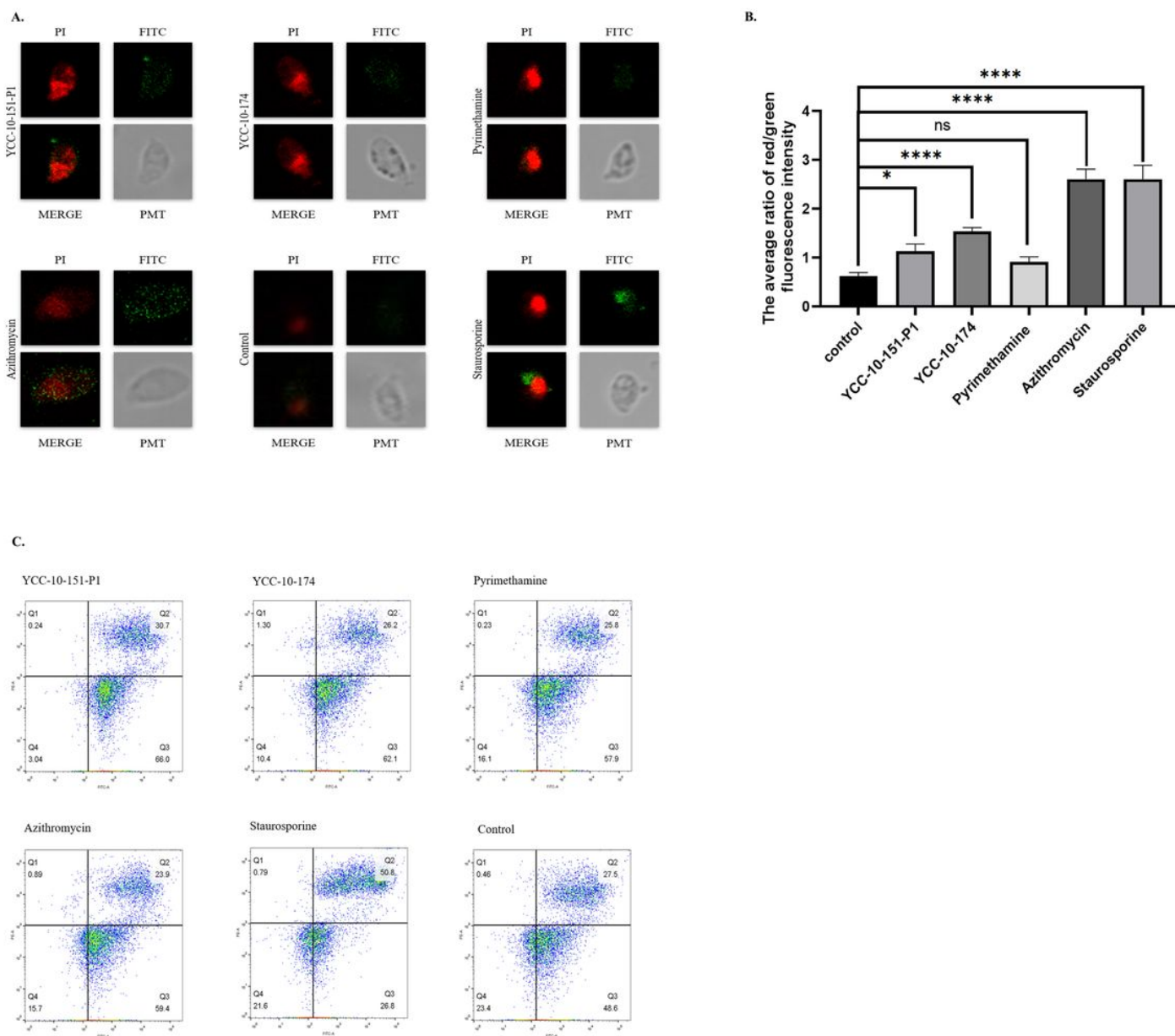


Figure 3

The death of RH tachyzoites induced by different stimuli. Fluorescent graphics (A), the average ratio of red and green fluorescence intensity (B) and flow cytometric analysis(C) of RH tachyzoites incubated with approximately IC_{50} of YCC-10-151-P1, YCC-10-174, pyrimethamine and azithromycin for 18 h. The results are shown as the means \pm standard error of the mean from independent experiments. *, $P < 0.05$. **** $P < 0.0001$. Abbreviations: FITC, green fluorescence; PI, red fluorescence; PMT (photomultiplier tube), light field with PMT as the detector and laser 488 nm as the light source.

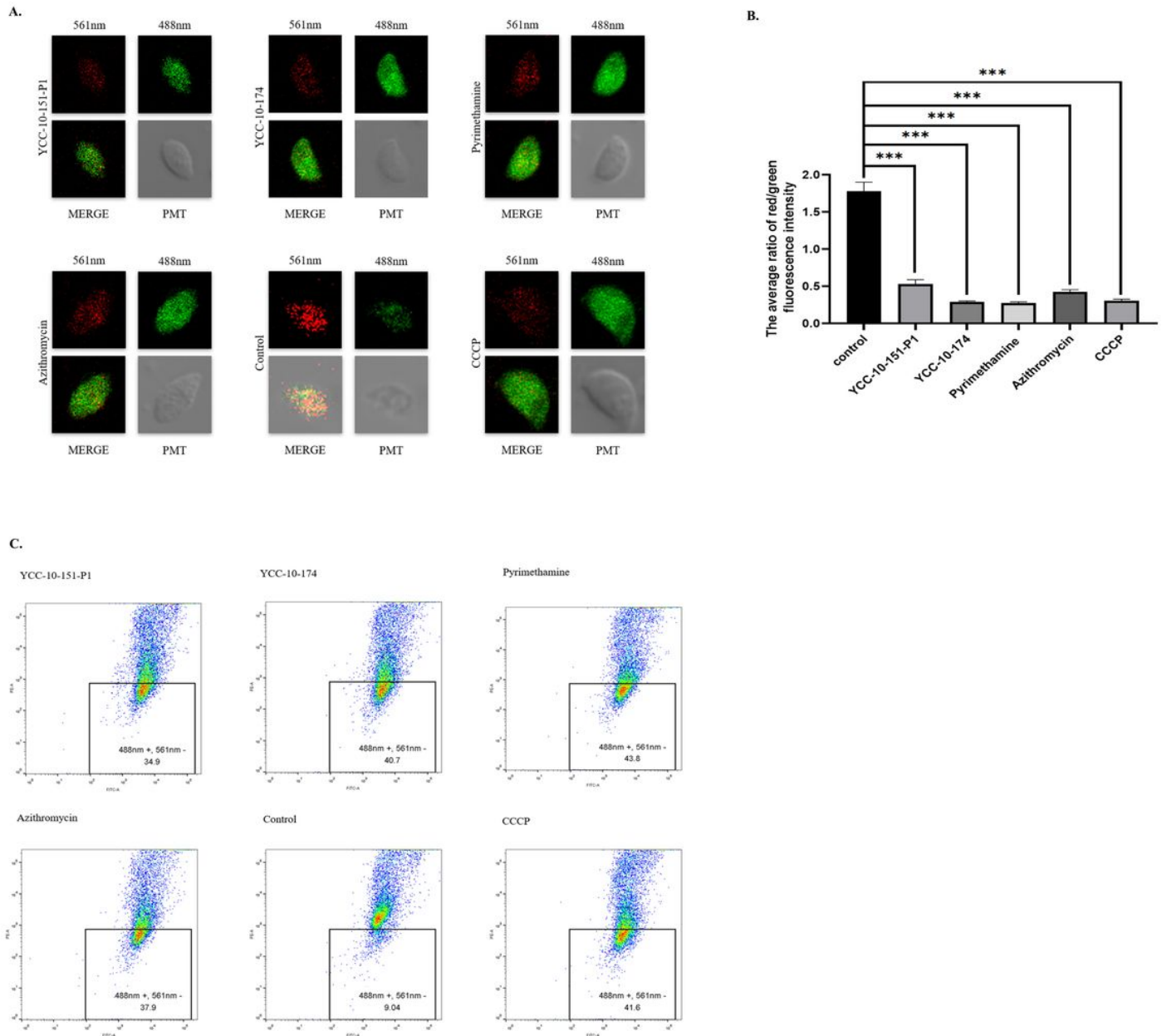


Figure 4

Depolarization of the RH tachyzoites mitochondrion. Confocal imaging(A), average ratio of red and green fluorescence intensity(B) and flow cytometric analysis(C) of tachyzoites treated with 500nM YCC-10-151-P1, 650nM YCC-10-174, 20 μ M pyrimethamine, 60nM azithromycin, 5 μ M CCCP and stained with JC-1. The results are shown as the means \pm standard error of the mean from independent experiments. *** $P < 0.001$.

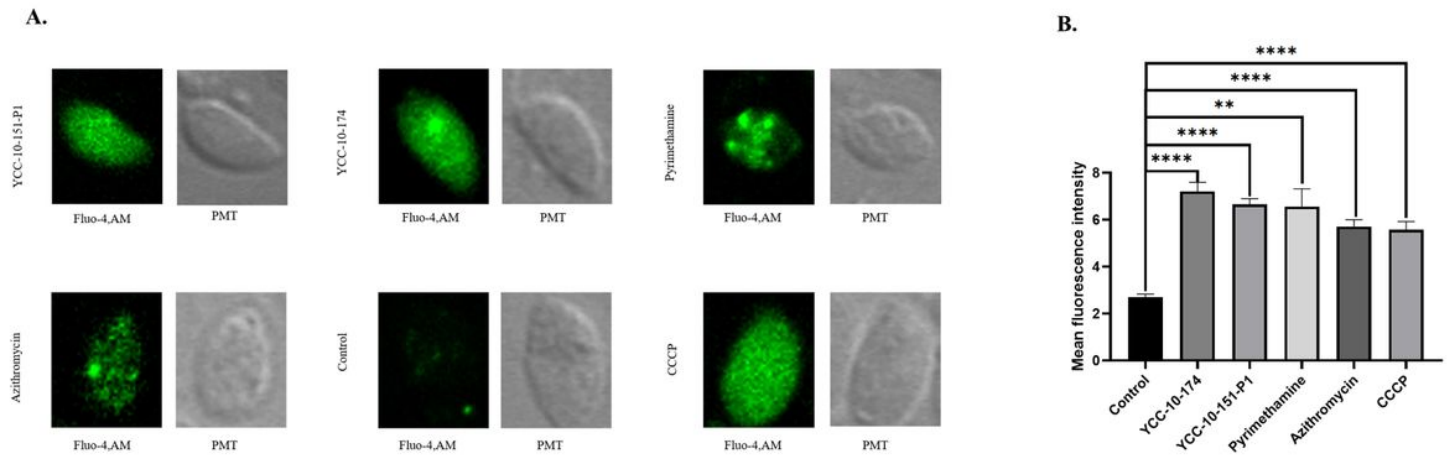


Figure 5

Elevation of intracellular Ca^{2+} levels. 500nM YCC-10-151-P1, 650nM YCC-10-174, 20 μM pyrimethamine, 60nM azithromycin and 5 μM CCCP were added directly into RH tachyzoites for 18h. (A) Observation of RH tachyzoites stained with Fluo-4 AM by confocal microscopy. (B) The analysis of the mean fluorescence intensity. The results are shown as the means \pm standard error of the mean from independent experiments. **, $P < 0.01$, **** $P < 0.0001$.

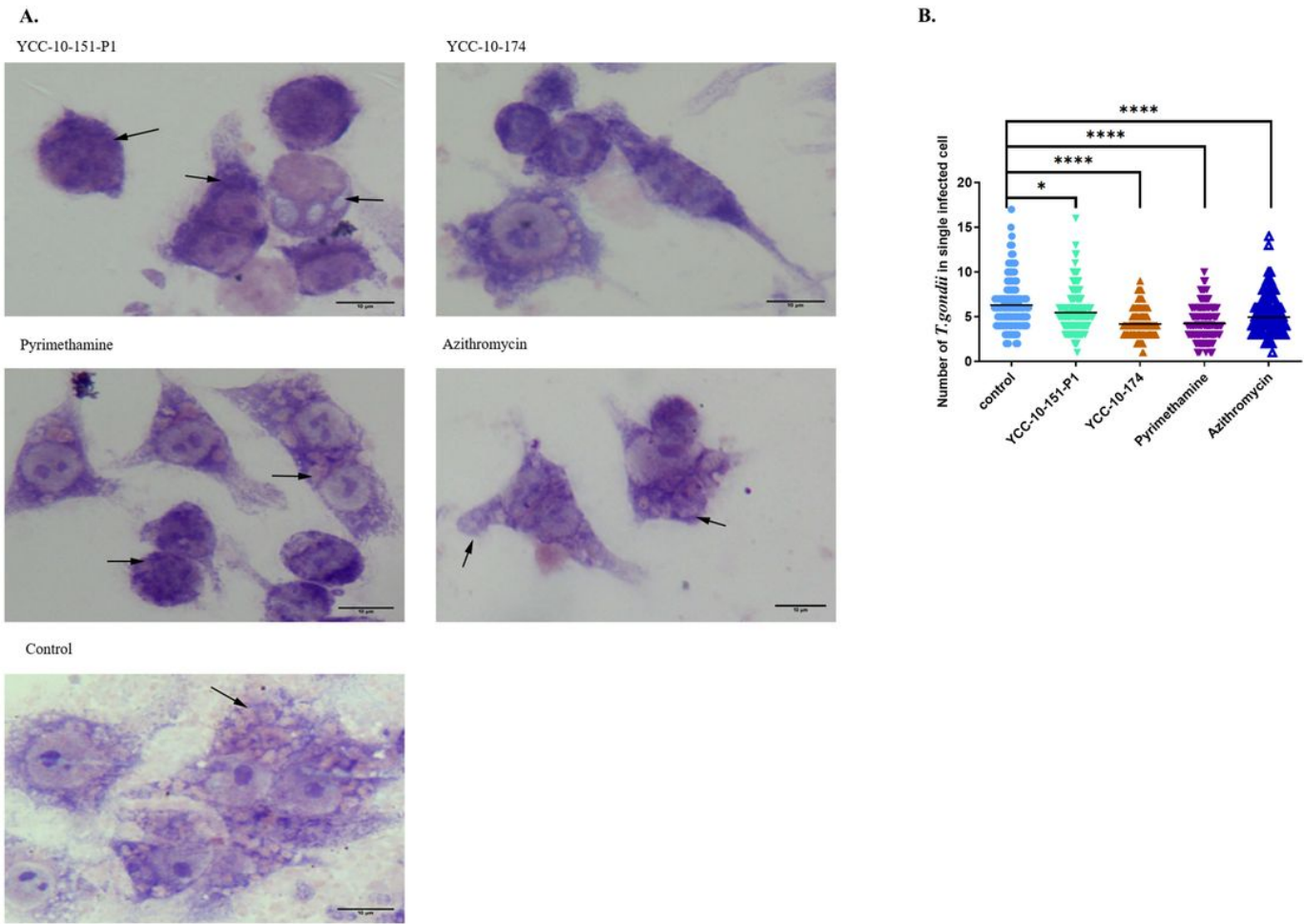


Figure 6

Invasion activity of RH tachyzoites after stimuli. (A)Wright's staining of tachyzoites invading macrophages after incubated with YCC-10-151-P1(500nM), YCC-10-174 (650nM), pyrimethamine(20 μ M) and azithromycin(60nM) for 18h. Black arrows, tachyzoites inside host cells. (B) A scattered distribution chart showing the means of the intracellular tachyzoite counts. Values represent actual numbers (scattered dots) and means (black line) from independent experiments; in each case, at least 200 infected cells were counted. *, P<0.5. ****, P <0.001.

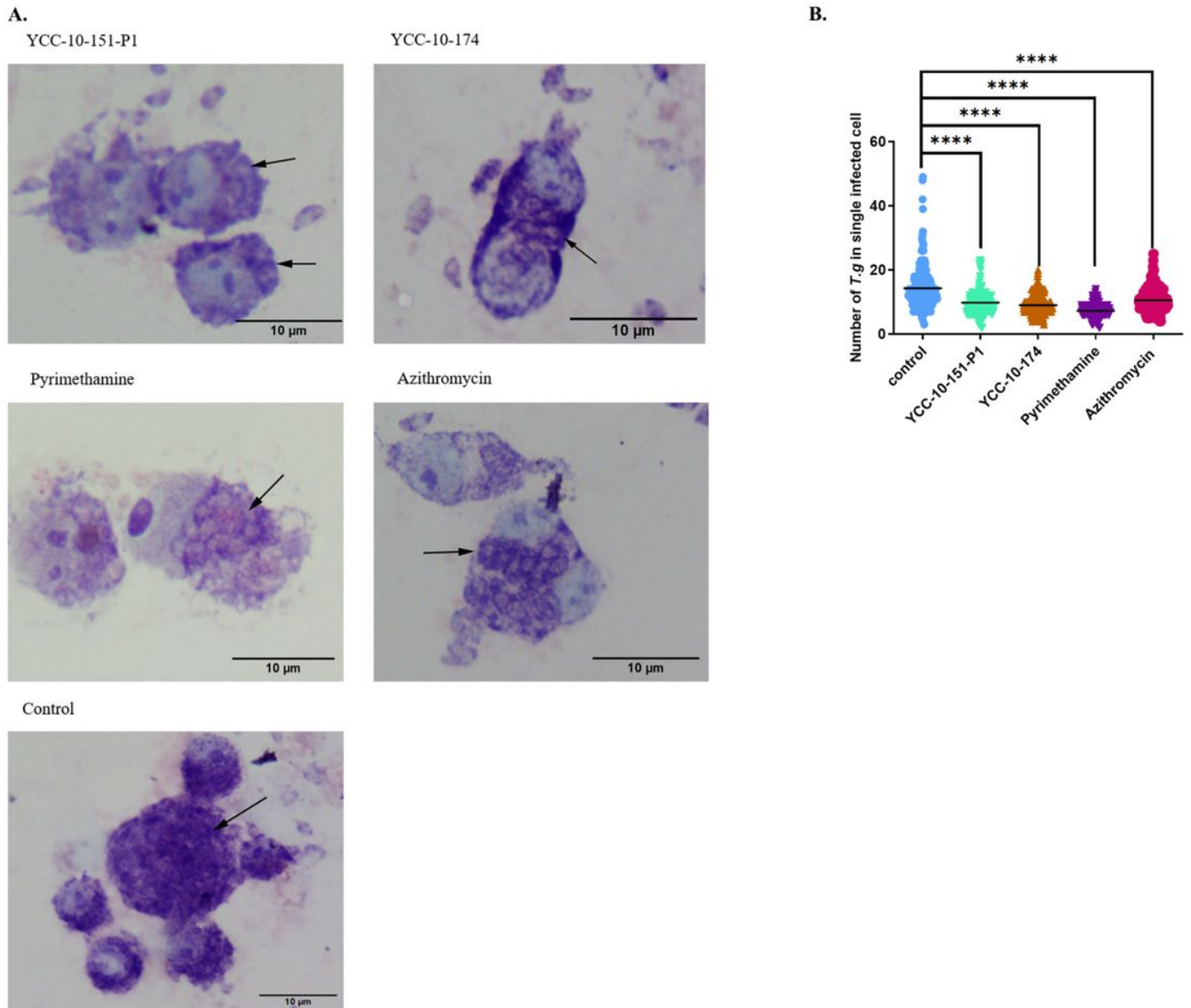


Figure 7

Intracellular growth of RH tachyzoites inside mouse macrophages with compounds *in vitro*. (A) Wright's staining of tachyzoites in macrophages after incubated with YCC-10-151-P1(500nM), YCC-10-174 (650nM), pyrimethamine(20μM) and azithromycin(60nM) for 36h. Black narrows, *T. gondii* tachyzoites. (B) A scattered distribution chart showing the means of the intracellular tachyzoite counts. Values represent actual numbers (scattered dots) and means (black line) from independent experiments; in each case, at least 200 infected cells were counted. T.g, *T. gondii* tachyzoites. ****, P <0.001.

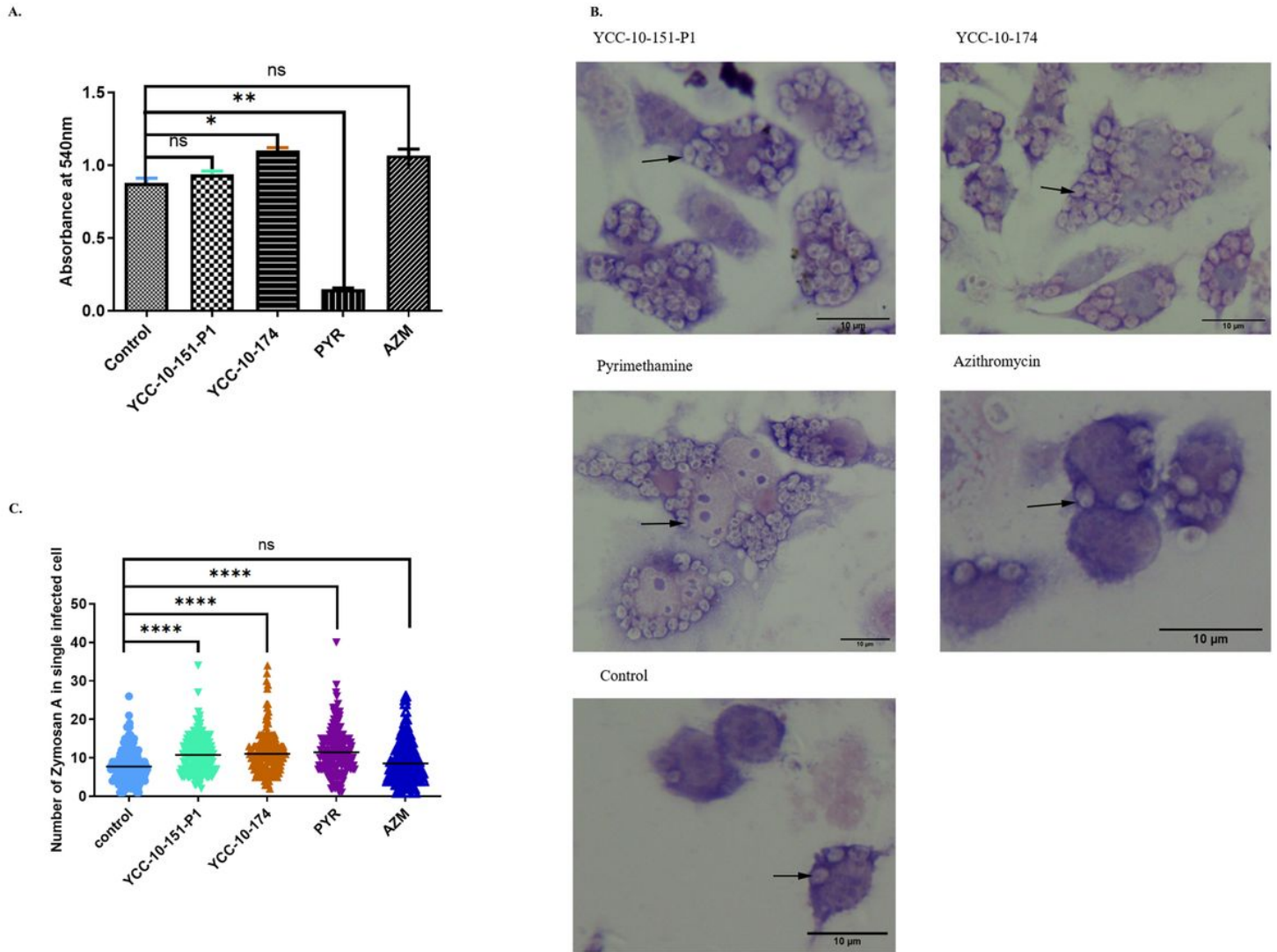


Figure 8

Lysosomal Activity and Phagocytosis of macrophages incubated with different stimuli. (A) The absorbance of neutral red at 540 nm. *, $P < 0.5$, 0.01 **, $P < 0.01$. (B) Wright staining of zymosan A particles in macrophages after 24h incubation with YCC-10-151-P1 (500nM), YCC-10-174 (650nM), pyrimethamine (20 μ M) and azithromycin (60nM). Black narrows, zymosan A particles. (C) The scattered distribution chart showing the means of the zymosan A particles counts. Values represent actual numbers (scattered dots) and means (black line) from independent experiments; in each case, at least 200 infected cells were counted. ****, $P < 0.001$